THE ENGINEERS'

BEACON

DIRECTOR'S NOTE

Dear Students,

"The spirit of engineering lies in innovation", with the same spirit, it gives me immense pleasure to present you all with the Students' Technical Consortium [STC] of SRM University, Chennai.

The aim of our university is to inspire and motivate the students to pursue their dream, capabilities and to reach their aim with full force. The right direction needs to be provided to students. SRM University being a multi streamed university has a lot to offer to the world. Workshops, research projects, competitions, fests, in addition to the college academics, all have a lot to play in developing the personality of a science and technology student. Apart from the expectations of the Industry, a student himself expects an environment which provides for this overall development opportunity.

Students' Technical Consortium is one such initiative to motivate and inspire the student institution towards the innovative knowledge, exchange and development.STC aims to provide students with a technical platform to find their talent and enhance their skills. The idea in itself is unique and and enhance their skills. The idea in itself is unique and exclusive. The first outcome of STC, the e-journal provides me with one more reason to be proud of the fact the first step has already been taken.

Happy reading to all the readers and to the great Isaac Newton's saying –"we build too many walls and less of bridges.", let us build a bridge to carry forward with our journey!

Dr. C. Muthamizhchelvan
Director, [E&T], SRM University
Chief Patron, STC

CONVENOR'S NOTE

Dear Students,

It gives me immense pleasure to write about the inauguration of Students' Technical Consortium [STC] of SRM University, Chennai.

I am delighted to share this message on this important occasion of initiating a bimonthly e-journal. The main mission of STC is to imbibe in students the spirit of innovation and harness their full potential.

We aim to create a milieu for seamless exchange of knowledge and the proliferation of scientific avenues in the best interest of the society and common person.

The journal is an excellent vehicle for sharing various events happening at various chapters and will enable us to learn from each other's experiences. STC can play a major role in bringing awareness among young generation and help in implementation of projects covering various domains of science and technology.

This initiative promises to be an exciting one, bringing together people from a range of disciplines to showcase research developments while providing a collegial atmosphere for scientific exchange. We have a stimulating technical program that boasts an array of highly regarded plenary and keynote speakers, drawn from all across the country.

A warm thank you must also be extended to our Director[E& T] and management for the unending support. Also, we thank the organizing committee for their commitment to this initiative which is greatly appreciated.

Wishing you a very productive academic year ahead and may we all be successful in bringing smiles to many more person on this planet.

Mr. A. Rathnam
Asst. Professor
Convenor, STC

FROM THE ORGANIZERS

It is our privilege to welcome the readers to explore the first edition of Students' Technical Consortium's e-journal: The Engineers' Beacon of SRM University, Chennai. It was really tenacious for us to compile this journal, distributing our work, sorting the articles, planning a whole new idea and executing it.With the right direction and guide provided by our Convenor and Director (E&T), we are now set to release for you all the first edition of The Engineers' Beacon

We have discussed and debated for months and agreed on the structure and working of the STC and with that the topics and nature of the contents of this journal. We tried our best to make this journal as informative as we could and with that we hope to give our readers a good reading experience.

Happy Reading!

Measurement of Mechanical Properties of Low Stress Silicon Nitride

Instructors : Gale Petrich: *Principal Research Scientist at Massachusetts Institute of Technology Past Research Scientist at Massachusetts Institute of Technology* Jurgen Michel :*Senior Research Scientist Microphotonics Center at Massachusetts Institute of Technology*, Scott J Poesse *Technical Instructor at MIT.*

Vijaya Rana : Student in *Department of Physics and Nanotechnology, SRM University, Chennai, India.*

***Abstract*- Low Stress Silicon nitride beams were fabricated to determine Young's modulus and residual stress of the thin film. The structures were mechanically loaded and the corresponding deflection was measured. From the load versus deflection curves, an effective spring constant was calculated. The spring constant was used to analytically determine a fundamental material property, the Youngs Modulus, of the silicon nitride. A decrement in the Youngs Modulus of the cantilever was observed and the percentage error found was approximately forty-four percentage. The value of the Residual Stress of thin films decreased from the expected value and the deviation was estimated to be twenty-two percent.**

***Index Term*-Youngs Modulus, Residual Stress, Silicon Nitride thin films.**

I. Introduction

THE evaluation of the mechanical properties of thin films is indispensable for designing Microsystems (MEMS) devices, since the properties are closely connected to the device performance. Elastic properties, such as Youngs Modulus, Poisson's ratio and shear modulus etc. are related to the functionality of the micro systems. The Youngs Modulus of the thin films is proportional to the stiffness of a device structure.

During the experiment Youngs Modulus and the Residual Stress of the low stress silicon nitride structures were determined. The structures were mechanically loaded and the corresponding deflection was measured. From the load versus deflection curves, an effective spring constant was calculated which is used to determine the Young's Modulus of the silicon nitride. The cantilever showed linear elastic behavior and the fixed -fixed beam varied in non-linear fashion. The Youngs Modulus determined was 146.42GPa and the residual stress was calculated to be 0.179 GPa. Analysis of these mechanical properties of the thin film of silicon nitride was done using a Hysitron TriboIndenter.

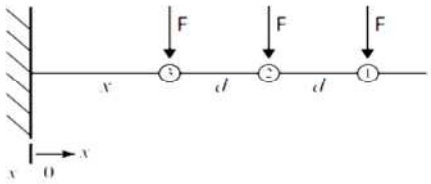

Fig.1. Force *F* being applied to the cantilever at three precisely separated locations for measuring the of the force constant *K* .

II. Experiment

II.a. Fabrication Process

The wafer was treated with Hexamethyldisilazane (HMDS) vapor followed by deposition of 4micron thick film of positive photoresist using the spin-on process. A hot plate at 90°C was used for the soft baking of the wafer. Then the wafer was exposed to Ultra-Violet light for 5 seconds using a mask aligner and subsequently post baking is done at 130°C for 5minutes. A microscope was used to inspect the wafers and for assessment of the overall result of photolithography. Dry-Etch of Silicon Nitride was done in plasma and Sulfur Hexafluoride. The photoresist was removed in the asher with the ashing time of 8 minutes per wafer. Silicon is etched in wet Potassium Hydroxide (KOH) bath at 80°C. Anisotropic etching of Silicon is done by addition of 20% KOH in 3 liters of (DI) Deionized Water. After KOH wet etching for 1-2 hours the wafer was rinsed again with Deionized Water (DI) water and sprayed with isopropanol. Isopropanol spray is used to avoid the stiction of the released cantilevers to the <111> side walls. The wafer was dried and the etching results were inspected under a microscope. A Diamond scribe was used to cut the wafer into individual groups, each of four dies.

II.b. Testing By Nanoindentation

The cantilever and fixed-fixed beams were mechanically tested to determine Youngs Modulus and the Residual Stress of the material. The structures were mechanically loaded and the corresponding deflection was measured. From the load versus deflection curves, an effective spring constant (k) was calculated as in Fig. (3) The spring constant was used to analytically determine a fundamental material property, the Young's Modulus, of the silicon nitride thin film.

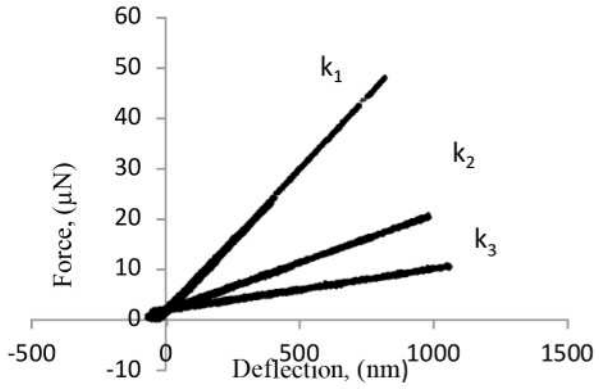

Fig.2.Force constants k_1=0.0571, k_2 =0.0192, and k_3 = 0.0082 is calculated by plotting Force versus Deflection.

The residual stress was calculated by plotting a graph between F/z and z, where F is the normal force and z is the deflection. Gradient of the straight line is influenced by the Youngs Modulus of the material while the Y- intercept gives information about the geometry and the residual stress of the structures.

III. Results and Discussions

The data from one force– deflection cycle was considered for the determination of the Youngs Modulus. The gradient of a F–z graph was assumed to be equal to $3EI/L^3$ for a long narrow beam, where F is the normal force acting on the beam, z is the deflection, E is the Youngs Modulus of the Silicon Nitride thin films and L is the length of the beam , I is the moment of inertia of the material, estimated by using $3EI/[(1-\nu^2)L^3]$, for a plate and by eliminating the offset from the force measurements. This method was straightforward, but because the position of the Nano indenter tip relative to the end of the beam was known to be within no fewer than a few micrometers, the estimate of E was a subject to substantial uncertainty.

A refined extraction approach was used to determine the spring constant $k = F/z$ of a beam at each of the three locations where the nanoindenter tip made contact with the beam. Graph was plotted between $k^{-1/3}$and L, the nominal distance from the cantilever's root to the location of the Nanoindenter tip. The gradient of the $(k^{-1/3})$–L graph was assumed to be equal to $(3EI)^{-1/3}$ for a beam or $[3EI/(1-\nu^2)]^{1/3}$ for a plate. In this way the uncertainty was reduced while extracting the value of Young's modulus. Where E is Young's modulus, ν is Poisson's ratio and z is the deflection, I is the moment of inertia w is the width and t is the thickness.

$$I = wt^3/12, \quad (1)$$

$$z = FL^3/3EI, \quad \text{for a long narrow beam,} \quad (2)$$

$$z = (1-\nu^2)\, F\, L^3/3E, \quad \text{for a plate.} \quad (3)$$

One cantilever, 50nm×100nm was tested, with a load F being applied to cantilever at three precisely separated locations. Force was applied at *10μm, 20 μm* and *30μm* away from the free end of the cantilever beam. The normal forces applied at three different points were *50μN, 100μN* and *200μN*. The force constant k was calculated by using $F=k\,x$, by plotting a graph of load versus displacement. The force constants k_1, k_2 and k_3 were calculated for the cantilever beam at the three different points of loading as shown in Fig. 2. The values of Force constants calculated is k_1=0.0571, k_2=0.0192, and k_3 =0.0082.Then graph was plotted against $(K)^{1/3}$ and x and the slope $b = (3EI)^{-1/3}$ was determined, as shown in Fig. 3. The Youngs modulus was calculated by using the formula

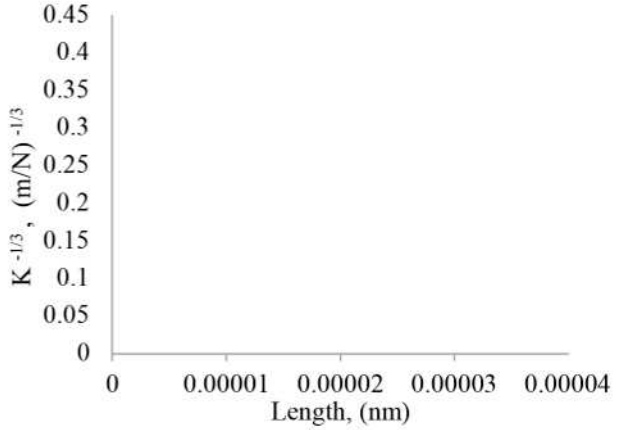

Fig.3. Graph is plotted between $K^{-1/3}$ and L, the gradient of the line is used to determine the Youngs Modulus by using $b = (3EI)^{-1/3}$. The Youngs Modulus is calculated to be 106.421GPa.

$$E = \frac{4}{wt^3b^3} \quad (4)$$

The Youngs Modulus for the cantilever beam was calculated to be 146.421GPa.

One of the fixed-fixed beams, 10nm ×50nm,of length L, width w and thickness t, with a residual stress in the film of σ_0 was loaded with force F at its center. The width was measured to be 8.39μm, the length was 49.μm and the thickness was around 1μm.The fixed-fixed beam was deflected and is loaded until the beam was fractured. The forces applied were 3000μN, 6000μN and 120000μN. The beam fracture occurred at 9000μN force. When a graph was plotted between F/z and z^2 a straight line was formed whose gradient depends on E and F/z intercept depends on geometry, E and residual stress. By using equation (5) the Residual stress was calculated to be 0.179 GPa. The force at the center is given as:

$$F = \left\{\left(\frac{\pi^2}{2}\right)\left[\frac{\sigma_0 wt}{L}\right] + \left(\frac{\pi^4}{6}\right)\left[\frac{Ewt^3}{L^3}\right]\right\}z + \left(\frac{\pi^4}{8}\right)\left[\frac{Ewt}{L^3}\right]z^3 \quad (5)$$

It was noted that the nominal beam 'width' of 10 μm was measured parallel to the edge of the etch pit. The bridges were oriented at an angle of arc tan (4/3) to the edges of the etch pits, so that the actual transverse width of this bridge (as it appeared on the photolithographic mask) was around 8μm. Berkovich indentation test was performed on SiN_x/Si wafers after deposition but before patterning or etching. Nano indenter tip was pressed into the film and the gradient of the force–displacement trace was used to estimate the reduced

modulus E_r, which is related to Young's modulus, E, of the material as follows:

$$\frac{1}{E_r} = \frac{(1-\nu^2)}{E} + \frac{(1-\nu_i^2)}{E_i} \qquad (6)$$

Equation(6) ν is Poisson's ratio of the SiN, E_i is Young's modulus of the diamond indenter tip (1100 GPa), and ν_i is Poisson's ratio of diamond (0.07).The maximum depth of indentation was ~70 nm. The value of the reduced modulus, averaged over 15 locations on the film, was 171.25 GPa.

TABLE I

THE YOUNGS MODULUS AND RESIDUAL STRESS VALUES WERE CALCULATED FOR THE 50nm×100nm CANTILEVER BEAM AND 10nm×50nm FIXED-FIXED BEAM RESPECTIVELY.

Results	Youngs Modulus	Residual Stress
Calculated Values	146.42 GPa	0.179 GPa
Expected Values	190±5GPa	0.342 GPa
% Error	44%	22%

In the tests the errors might have occurred due to the inaccuracy in determination of the beam and the test geometry. Some drawbacks would have arisen due to effect of the substrate properties of the Nano indenter during testing. The deviation in the value of Youngs Modulus was possibly due to the non-uniformity of the LPCVD (Low -Pressure Chemical Vapor Deposition) Silicon Nitride thin film, as was observed by the change of the reflected color across the wafer. The decrease in the Residual stress value was reported due to the high temperature deposition conditions. Thermal stress was produced due to the difference in the expansion coefficient of Silicon and Silicon Nitride, subsequently decreasing the Residual Stress of the Si on SiN_x. The film growth mechanism and the amorphous nature of the film might have also contributed to the variation in the values of the Youngs Modulus and the Residual Stress.

IV. Conclusion

The Youngs Modulus measurement of the low stress Silicon Nitride structures have been performed by plotting load versus deflection graph and was calculated to be 146.42 GPa. There was decrement in the Youngs Modulus and the deviation was approximately 44%. Linear behavior of the force and the displacement curve was observed for the (50nm×100nm) cantilever and non-linear for the (10nm×100nm) fixed-fixed beams. The thin film's residual stress was determined as 0.179 GPa and the percentage error was estimated to be 22%.

Acknowledgememt

The authors would like to thank the staff of Micro/Nanoprocessing, 6.152J in Massachusetts Institute of Technology for their help and support in the project.

References

[1]W. H. Chuang, T. Luger,R.K. Fettig, R.Ghodssi, Member,IEEE, "Mechanical Property Chracterisation of LPCVD Silicon Nitride Thin Films at Cryogenic Temperature", *Journal of Microelectromechanical Systems,* vol. 13, no .5, p.870, 2004.

[2]J.Mencik and E.Quandt "Determination of Elastic Modulus of Thin films and specimens using bending methods", *Journal of Materials Research,* vol. 14, no. 5, p. 2152-2154, 1999.

[3]M.W. Denhoff "Measurement of Youngs Modulus and Residual Stress in MEMS bridges using a surface profiler", *Journal of Micromechanics and Microengineering,* vol. 13, p. 691, 2003.

[4]H.Guo and A.Lal "Die level Characterization of Silicon Nitride Membrane/Silicon Structure using Resonant Ultrasonic spectroscopy", *Journal of Microelectro-mechanical Systems,* vol. 12, no. 1, p. 55, 2003[5]C.K.Fedder "MEMS Fabrication", *International Test Conference,* paper 27.3, p. 14, 2003.

[6]W.N.Sharpe, K.J.Hemker, R.L.Edwards, "Mechanical Properties of MEMS Materials" *Defense Advanced Research Projects Agency,* Financial Technical Report, order no. J346, p. 33, 2004

[7]V.T.Srikar, S.M. Spearing "A critical Review of Micro scale Mechanical Testing Methods used in the design of Microelectromechanical Systems", *Society for Experimental Mechanics,* vol. 43, no. 3, p. 238-241, 2003.

SMA Based Camera Gimbal for Point/Trajectory Tracking

Karan Vaish and Rakesh Vasireddy

***Abstract*—As evident, the camera has largely varied applications. The advancements in technology beckon the need for development of optimized control systems. Such a control system is presented, based on transformation of grids/planes and shape memory alloys that prove to be much lighter and faster, thus enabling the use of cameras in areas that are presently found hard. Two linear actuators based on 2-way, step wise actuated, SMAs are coupled together to accurately position one end of a lever, on a plane, that moves the camera mounted at the other end of the lever, with the longer arm, in a spherical plane. The larger spherical plane of the camera is transformed into a much smaller, control plane (planar) of the SMAs using appropriate transformation techniques leading to, apart from a single point, tracing of complex curves with extremely high angular velocities. The large force to weight ratio of an SMA makes the control system extremely light and low power consuming than servo motors, even for relatively heavy cameras. For example, in robotic eyes, motion analysis of objects with known trajectories, so on and so forth.**

***Index Terms*—SMAs, cameras, actuators.**

I. Introduction

The basic concept of operation aims at reduction in the size of the control plane, and production of magnified results. Using the desired difference in lengths on the either side of the fulcrum, in a simple three dimensional lever system, very little movement of the control arm leads to proportionately large angular deflections of the camera mount. The movement of the control arm is actuated by linear, stepped actuators based on shape memory alloys. The step wise actuations are obtained by the use of electrical taps at different lengths of the actuator thus energizing only small parts leading to a stepped linear extension. First we will discuss what are shape memory alloys and their properties, how they work. Moving on we shall present the assembly of our components and how exactly are they meshed with each other. Then we shall proceed to the discussion of the link between the physical space and the control space, followed by appropriate transformation techniques and software integration. This is where the complete concept of operations have been explained.

II. Shape Memory Alloys

A shape-memory alloy (SMA, smart metal, memory metal, muscle wire, smart alloy) is an alloy that "remembers" its original, cold-forged shape: returning to the pre-deformed shape when heated. This material is a lightweight, solid-state alternative to conventional actuators. Shape-memory alloys have different shape-memory effects. Two common effects are one-way and two-way shape memory.

One-way memory effect is when a shape-memory alloy is in its cold state (below A_s), the metal can be bent or stretched and will hold those shapes until heated above the transition temperature. Upon heating, the shape changes to its original. When the metal cools again it will remain in the hot shape, until deformed again. The two-way shape-memory effect is the effect that the material remembers two different shapes: one at low temperatures, and one at the high-temperature shape. A material that shows a shape-memory effect during both heating and cooling is called two-way shape memory. This can also be obtained without the application of an external force (intrinsic two-way effect). The two main types of shape-memory alloys are copper-aluminium-nickel, and nickel-titanium (NiTi) alloys but SMAs can also be created by alloying zinc, copper, gold and iron. NiTi alloys are generally more expensive and change from austenite to martensite upon cooling [1]. The three main SMA phases are shown in Fig. 1.

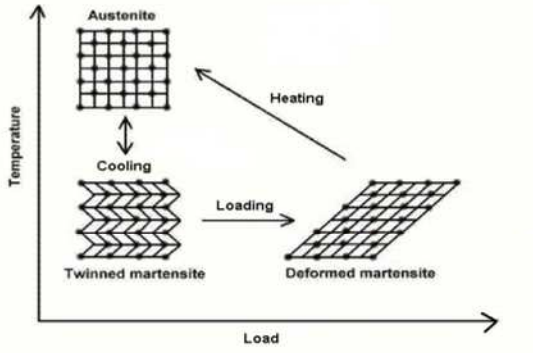

Fig. 1. SMA phases

III. Assembly

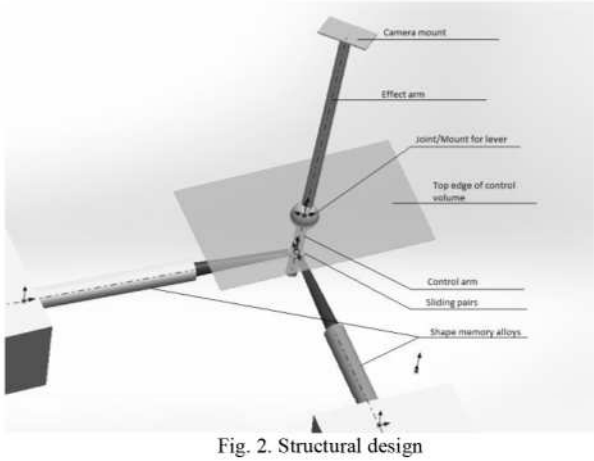

Fig. 2. Structural design

1) As shown in Fig. 2 the two shape memory alloys are mounted perpendicularly to each other with a rotational degree of freedom in the same plane. They both are

connected to the control arm (shorter arm) of the lever using sliding pairs. The lever is mounted on the control volume using a simple ball socket joint configuration with the effect arm (longer arm with the camera mount), protruding out of the control volume. The camera is fixed on the mount.

2) Smaller is the length of control arm, greater is the angular deflection (Θ).
Let length of control arm at neutral position (perpendicular to the top surface) = '*a*' *mm*
Maximum amount of extension possible by the SMA = '*2l*' *mm.*
Using simple trigonometry,

$$\Theta = \tan^{-1} l/a. \quad (1)$$

3) Smaller is the ratio of control arm length to effect arm length, greater is the linear force required.
Let the length of the effect arm = *'b' mm*
Let the weight of the camera = *'w' kg*

$$F = w \times (b/a) \text{ Newtons.} \quad (2)$$

IV. Transformations

Each Coordinate on the effect plane, where the camera needs to be pointed at (taken as an input from the user) has a complimentary coordinate on the control plane as shown in Fig. 3. This coordinate relationship can be determined by simple geometric equations given below, where (*X*, *Y*, *Z*) are notations for the effect plane and (*x*, *y*, *z*) are the notations for the control plane. The origin is placed at the points where the line, perpendicular to the control plane and passing through the centre of the ball socket joint intersect the two (effect and control) planes.

$$X = -b \times \left[1 - \frac{a}{\sqrt{a^2+y^2}}\right] \quad (3)$$

$$Y = b \times y \div \sqrt{a^2 + y^2} \quad (4)$$

$$Z = b \times z \div \sqrt{a^2 + z^2} \quad (5)$$

Similarly every single curve drawn on the effect plane will have a complementary curve on the control plane. The trajectory/curve can be found out by simply substituting the complementary points in terms of *x*, *y*, *z* in place of *X*, *Y*, *Z* in the equation.

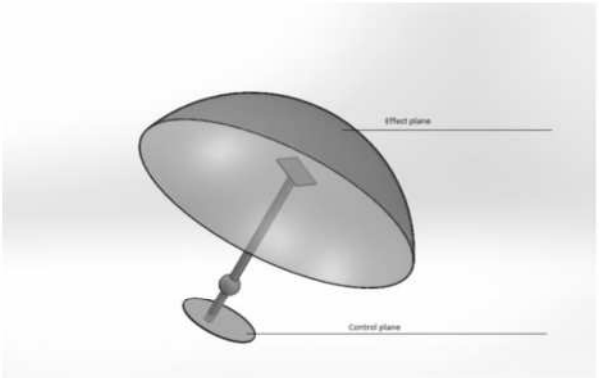

Fig. 3. Effect plane and control plane

For greater accuracy in tracing trajectories a different approach is required. Since the input is being taken in reference to the position of the camera, for simplicity, it is important that the effect plane stays a simple two dimensional Cartesian plane (Fig. 4) while transformation techniques are employed to generate a completely different non linear two dimensional grid for the control plane (Fig. 5) . This non-uniform scaling originates from the fact that the camera follows a curved path while the physical space is assumed to be planar. Hence for accurate positioning transformation between following grids is employed.

Numerous techniques can be employed for these types of transformations. A simple method for grid transformation is shown as follows

$$X' = x_o + a_1X + a_2Y + a_3XY + a_4X^2 + a_5Y^2 + a_6X^2Y + a_7XY^2 + a_8X^3 + \quad (6)$$

$$Y' = y_o + b_1X + b_2Y + b_3XY + b_4X^2 + b_5Y^2 + b_6X^2Y + b_7XY^2 + b_8X^3 + .. (7)$$

Equation (6) and (7) show a type *of simple projective* transformation which is non-linear and relates two 2D Cartesian coordinate systems through a *translation,* a *rotation* and a *variable scale change*. The transformation function can have an infinite number of terms [2]. Other methods include various discretization techniques [3] that are beyond the scope of this paper.

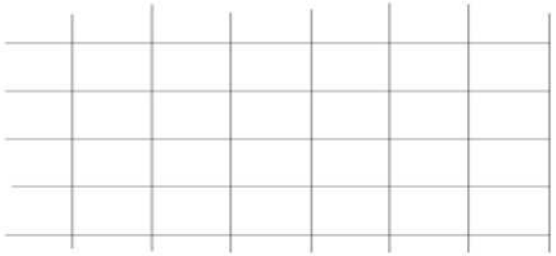

Fig. 4. Effect plane (cartesian plane)

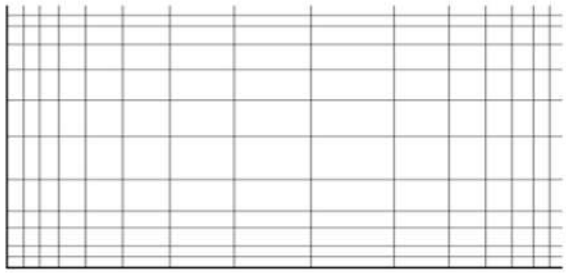

Fig. 5. Control plane

V. Controller Design

The primary challenge in precisely controlling SMAs is their highly nonlinear hysteretic transformation, material degradation, and thermo-mechanic fatigue. While all these complexities come from SMA materials' components characteristic and SMA actuator's geometry. This brings fundamental concerns that for different materials, shapes and geometries of the devised SMA actuator, the deformation mechanisms, temperature-induced phase transformation properties, hysteresis loops, and thermo-mechanics fatigue characters will be un-doubtfully different. A simple SMA controller design has been shown in Fig. 3 based on a closed loop approach and adaptive tuning [4].

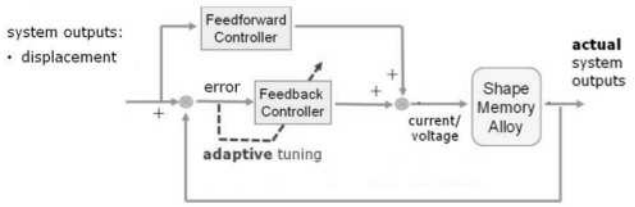

Fig. 6. SMA control system

A. Actuation

SMA actuators are typically actuated electrically, where an electric current results in Joule heating. Deactivation typically occurs by free convective heat transfer to the ambient environment. Consequently, SMA actuation is typically asymmetric, with a relatively fast actuation time and a slow de-actuation time. A number of methods have been proposed to reduce SMA deactivation time, including forced convection, and lagging the SMA with a conductive material in order to manipulate the heat transfer rate.

Novel methods to enhance the feasibility of SMA actuators include the use of a conductive "lagging" [5]. This method uses a thermal paste to rapidly transfer heat from the SMA by conduction. This heat is then more readily transferred to the environment by convection as the outer radii (and heat transfer area) is significantly greater than for the bare wire. This method results in a significant reduction in deactivation time and a symmetric activation profile. As a consequence of the increased heat transfer rate, the required current to achieve a given actuation force is increased.

TABLE I: CURRENT CHARACTERISTICS OF SAMPLE SMA

Diameter Size (Inches)	Resistance (Ohms/ Inch)	Maximum Pull Force (grams)	Approximate* Current at Room Temperature (mA)	Contraction* Time (seconds)	Off Time LT=70° C Wire** (seconds)	Off Time HT=90° C Wire** (seconds)
0.0010	45.0	7	20	1	0.10	0.06
0.0015	21.0	17	30	1	0.25	0.09
0.002	12.0	35	50	1	0.3	0.1
0.003	5.0	80	100	1	0.5	0.2
0.004	3.0	150	180	1	0.8	0.4
0.005	1.8	230	250	1	1.6	0.9
0.006	1.3	330	400	1	2.0	1.2
0.008	0.8	590	610	1	3.5	2.2
0.010	0.5	930	1000	1	5.5	3.5
0.012	0.33	1250	1750	1	8.0	6.0
0.015	0.2	2000	2750	1	13.0	10.0
0.020	0.16	3562	4000	1	17.0	14.0

B. Stepwise Actuation and Positional Feedback

The actuation of the SMA can be carried out in a stepwise fashion rather than the usual ON-OFF approach. The advantage of this method lies in the precision and controlled actuation lengths that can be achieved. This also increases the resolution of the mapped Cartesian plane as smaller stroke lengths can be achieved by this method. The positional control system for the shape memory alloy (SMA) wire actuator uses an electrical resistance feedback. A control scheme is implemented to eliminate the need for a position sensor to achieve stable and accurate positioning by utilizing the actuator's electrical resistance feedback [6]. The main bottle neck for this approach is the non-linear behavior of the SMA material which results in small variations in resistance for a given length. This can be solved by employing artificial intelligent systems like neural networks or fuzzy logic based systems. The control system can further be improved by using a proportional-derivative (PD) based approach to attain optimum response [7].

VI. SOFTWARE - USER INTERFACE AND THE PROCESS

The inputs to the system are given by the user whose primary objective is to trace the trajectory of a body. This can be done in two ways. The user can either input the co-ordinates where the camera has to be focused or moved to. Alternatively the user can also input equations of trajectories the camera can automatically trace without further inputs from the user end. The software design consists of a GUI (graphical user interface) where the inputs from the user are taken. These inputs are processed accordingly based on the type of trajectory. The most commonly used trajectories like circular, oval, parabolic, elliptical, hyperbolic etc... are pre-transformed into their planar equations by using appropriate transformation equations which have been explained in the Transformations section above. These transformed planar equations are used to extract the co-ordinates of the trace points on the control plane. Depending on these planar co-ordinates the stroke length of individual SMAs can be calculated. Once this is done the electrical actuation system explained in the above sections is used to obtain the required output by precise Joule heating. This process is repeated again and again to trace all the co-ordinates on the control plane there by making the camera move in the required trajectory .

VII. CONCLUSION

The above discussed mechanism can be used to obtain a lighter, low power consuming, and a much faster control system for cameras. These cameras can then also be used for motion analysis of various objects with known trajectories done in controlled environments. This is possible only because of extremely higher angular accelerations achievable by the presented mechanism. This mechanism may be the ideal choice to replace traditional gimbal setups as camera mounts on UAVs as they offer more optimized performance in terms of weight and power that play a vital role in deciding the characteristics of a plane.

REFERENCES

[1] D. E. Ming and W. H. Biermann, "Shape Memory Alloys Hodgson," R *JASM International, Metals Handbook*, Tenth Edition. Vol. 2. Properties and Selection: Nonferrous Alloys and Special-Purpose Materials, pp. 897-902, 1990.

[2] K. T. Tang, "Mathematical Methods for Engineers and Scientists," Springer, vol. 2, pp. 13, 2006.

[3] V. D. Liseikin, "A Computational Differential Geometry Approach to Grid Generation," Springer, pp. 38, 2007.

[4] C. A. Dickenson and J. T. Wen, "Feedback control using shape memory alloy actuators," *Journal Of Intelligent Material Systems and Structures*, vol. 9, April 1998.

[5] S. Huang, M. Leary, T. Attalla, K. Probst, and A. Subic, "Optimization of Ni–Ti shape memory alloy response time by transient heat transfer analysis," *Materials & Design*, vol. 35, pp. 655–663, 2012.

[6] N. Ma, G. Song, and H. J. Lee, "Position control of shape memory alloy actuators with internal electrical resistance feedback using neural networks," *IOP Science, Smart materials and Structures*, vol. 13, no. 4.

[7] Y. J. Lee, H. M. son , J. B. Gu , and T. H. Nam, "Design and control of multistep SMA actuator," *E-MRS fall meeting*, 2005.

An Efficient Ferrocene Derivative as a Chromogenic, Optical, and Electrochemical Receptor for Selective Recognition of Lead(II)in an Aqueous Environment

Vijaya Rana : *Department of Physics and Nanotechnology, SRM University, Chennai, India.*

Abstract- **Triazolyl Fischer carbine complexes of ferrocene derivative 3 synthesised by the regioselective [3+2] cycloaddition reaction of azides with alkynyl Fischer carbene complexes. The cation complexation properties of these ferrocene derivatives have been studied using electrochemical and spectroscopic techniques. The exceptional structural features existing in these receptors are the presence of Fischer carbene complex, connected to 1-position of the ferrocene center through 1,2,3 triazole ring. The receptor 3 experiences perturbation of the CV in presence of Pb^{2+} with a change of electrochemical potential (the anodic shift $\Delta E_{1/2}$ = 55 mV for 3).**

The changes in the absorption spectra are accompanied by the appearance of a new high energy (HE) peak at λ = 206 nm ($2742 \times 10^2\ M^{-1}cm^{-1}$) and the absorption band centered at 240 nm is decreased. During the titration two isosbestic points around 226, and 255 nm were observed(Fig.4) indicating that only one spectrally distinct 3-Pb^{2+} complex was formed.

The receptors show colorimetric response and act as a selective "turn off" chemical receptor for the Pb^{2+} ion

I INTRODUCTION

The development of selective and sensitive imaging tools capable of monitoring heavy- and transition-metal ions has attracted interest because of their wide use in various fields of science and the subsequent effects of these metals in the environment and nature. Among the heavy metals, Pb^{2+} ion is one of the most toxic metal ions and is often encountered due to its wide distribution in the atmosphere as well as its current and previous use in batteries, gasoline, and pigments. The accumulation of lead in the body can result in neurological, reproductive, cardiovascular, and developmental disorders. As a result, the development of new methods for the sensitive and selective detection of Pb^{2+} is highly desirable.

However, the design and the advancement of new and practical chemosensors, which offer a promising advance for Lead ion detection, is still a great challenge in supramolecular chemistry. As a result, the development of good sensors for the detection of these toxic metal cations through multiple exhibiting physical responses upon coordination of Pb^{+2} have been reported. One of the most elegant ways of achieving sensor design is to functionalize a receptor capable of both selective substrate binding with a metal cation and reporting on the recognition event through a variety of physical responses. Such Lead sensors should display high solubility in water and a high selectivity for Lead ions against a background of challenging analytes. However, most of these molecules have limitations due to the interference from other contending metal ions as well as low water solubility. As a result, not many molecules are known that selectively sense Lead ion in aqueous environment.

The versatility and utility of Fischer carbene complexes have been widely demonstrated during the past two decades.The rich and diverse chemistry of these complexes has been utilized as key steps in the synthesis of several natural products.Especially rewarding has been their participation in various cycloaddition reactions,the products of which usually retain the metal carbene functionality that can be utilized in further transformations.Thus, from a synthetic standpoint, ferrocene is a very attractive building block for redox-active ligands because of the robustness of ferrocene under aerobic conditions and the ease of functionalization. These facts, coupled with its electrochemical and UV−vis spectroscopic properties, which can be perturbed by the proximity of bound guests, reveal that ferrocene is an important functional tentacle in this research area.

In this context, the design of redox-active receptors in which a change in electrochemical behavior can be used to monitor complexations of guest species is an increasingly important area of molecular recognition. With a vision to advancing chemical sensor technology, considerable interest is being shown in the synthesis of redoxactive receptors that contain a redox center. In ferrocene derivatives, cation binding at an adjacent receptor site induces a positive shift in the redox potential of the ferrocene/ferrocenium redox couple, and the complexation ability of the ligand can be switched on and off by varying the applied electrochemical potential. The magnitude of the electrochemical shift (ΔE1/2) upon complexation represents a quantitative measure of the

perturbation of the redox center induced by complexation to the receptor unit. In this report a practical protocol for [3+2] cycloaddition of ferrocenyl azide with alkenyl Fischer carbine complex leading to triazolyl Fischer carbene complex has been demonstrated.

II EXPERIMENTAL SECTION

Ia.CHEMICALSANDGENERALMETHOD

Appropriate salts of Na^+, K^+, Li^+, Tl^+, Ca^{2+}, Mg^{2+}, Mn^{2+}, Cr^{2+}, Fe^{2+}, Co^{2+}, Cu^{2+}, Zn^{2+}, Cd^{2+}, Ni^{2+}, Hg^{2+} and Pb^{2+}, 1-pyrenecarboxaldehyde,n-butyllithium, 1,8-diazabicyclo[5.4.0] undec-7-ene (DBU), copper iodide (CuI) were purchased from Aldrich and directly used. Sodium azide, sodium borohydride, acetonitrile (HPLC), diethyl ether, was purchased from local chemicals.As shown in Scheme (azidomethyl) ferrocene, **1** undergoes "[3+2] cycloaddition reaction with Alkenyl fiischer carbene complex to give triazolyl fischer carbene complex**3** ($C_{23}H_{21}O_6N_3FeW$).

Column chromatography was carried out on 3 cm of silica gel in a column of 2.5 cm diameter using 100-200 mesh silica gel. All solvents were dried by conventional methods and distilled under Ar atmosphere before use. As shown in Scheme (azidomethyl) ferrocene, **1** undergoes "[3+2] cycloaddition reaction with Alkenyl fiischer carbene complex to give triazolyl fischer carbene complex **3** ($C_{23}H_{21}O_6N_3FeW$), the compound **3**. UV-vis spectra were taken in CH_3CN solutions at $c = 1 \times 10^{-5}$ M. Cyclicvoltammetry (CV) was performed with a conventional three-electrode configuration (glassy carbon as working electrode, platinum as auxiliary electrode and Ag/Ag+ as reference electrode). The experiments were carried out with 10^{-4} M sample solution in CH_3CN using [$(n\text{-}C_4H_9)_4NClO_4$] (TBAP) as supporting electrolyte, after de-oxygenation of the solution. Working electrode was cleaned at the end of each run. Cyclic voltammograms were recorded at a scan rate 0.1 Vs^{-1}.

I.bINSTRUMENTATION

The ^1H, ^{13}C NMR spectra were recorded on Bruker 400, 500 MHz FT-NMR spectrometers, using tetramethylsilane as the internal reference. Electrospray ionization mass spectrometry (ESI-MS) measurements were carried out on a Qtof Micro YA263 HRMS instrument. The absorption spectra were recorded with a JASCO V-650 UV-vis spectrophotometer at 298K. The CV measurements were performed on a CH potentiostat model CHI630D.

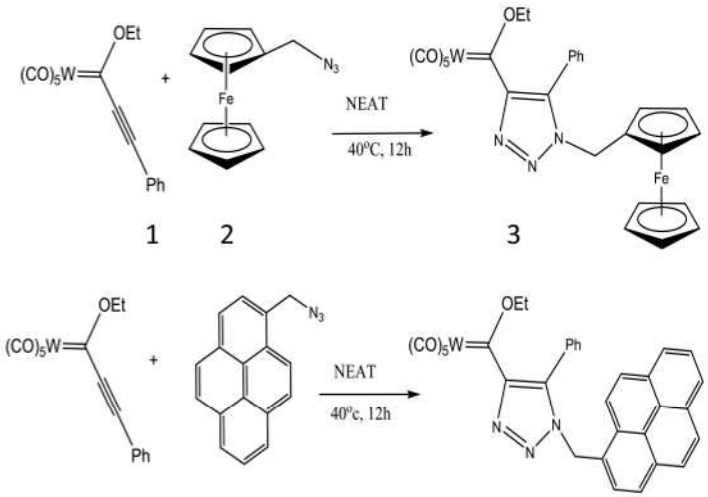

Fig.1. Scheme 1. Synthesis of ferrocene receptors 3using [3+2]cycloaddition reaction.

***Cautions**: Due to explosive nature of Metal-perchlorates in certain conditions, precautions should be taken to handle perchlorate salts!*

I.c. SYNTHESIS OF COMPOUND 3

Fischer carbene complex(1.0 eq) and ferrocenyl monoazide (1.5 eq) were taken in a two neck r.b. and thoroughly degassed with argon. The reaction mixture was stirred at 40°c for 12h product was purified using silica gel column chromatography. Elution with EtOAc/hexane(1:9, v/v) yielded **3** (0.34g) and progress of the reaction was monitored by TLC.

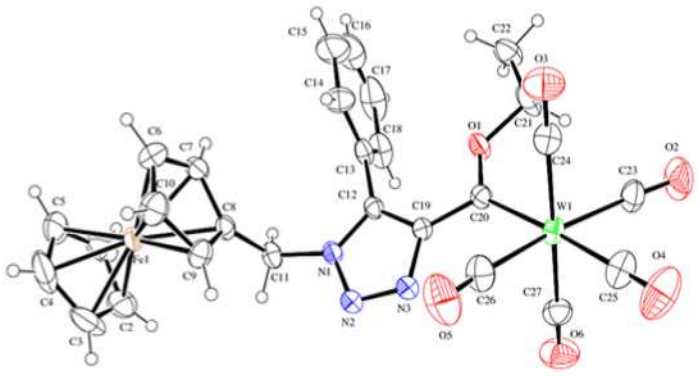

Fig.3. Molecular structure of 3 with thermal ellipsoid drawn at the 30% probability l

II. RESULTS AND DISCUSSIONS

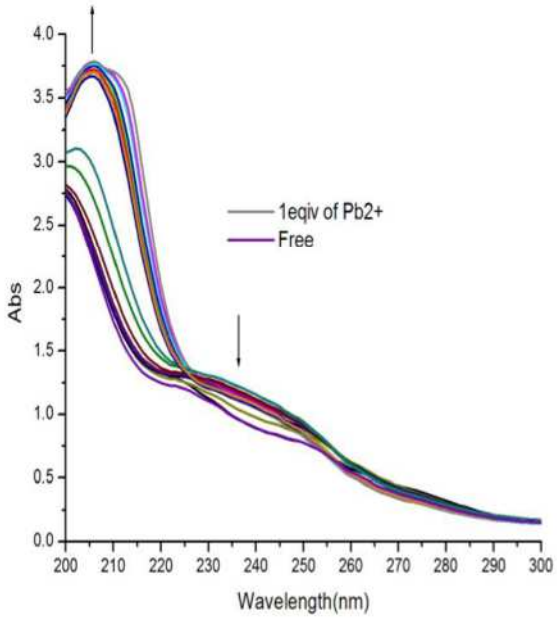

Fig.5 UV-vis absorbance spectra of 3 (10^{-5} M) upon addition of different metal cations up to 1 equiv in CH_3CN/H_2O (5/5)

II a. UV-VIS ABSORPTION STUDIES

The UV−vis binding interaction studies of receptor **3** was performed in (CH_3CN/H_2O, 5/5) (1×10^{-5} M) against cations of environmental relevance, such as Li^+, Na^+, K^+, Ag^+, Ca^{2+}, Mg^{2+}, Cr^{2+}, Zn^{2+}, Ni^{2+}, Co^{2+}, Fe^{2+}, Tl^+, Hg^{2+}, Cd^{2+} and Pb^{2+} as perchlorate salts. The compound **3** show absorption response in presence of Pb^{2+} ion. The change in the UV−vis absorbance spectra of receptors **3** in (CH_3CN/H_2O, 5/5) due to the stepwise addition of Pb^{2+} ion are shown in Figure 1. Upon gradual addition of 1 equiv of Pb^{2+} to **3**, the high-energy (HE) absorption band at λ = 206 nm (2742×10^2 $M^{-1}cm^{-1}$) and the absorption band centered at 240 nm , decreased. During the titration two isosbestic points around 226, and 255 nm were observed(Fig.1) indicating that only one spectrally distinct **3**-Pb^{2+} complex was formed.The binding assays using the method of continuous variations (Job's plot) suggest 1:1 (cation/receptor) complex formation with Pb^{2+} ion for compounds **3**.

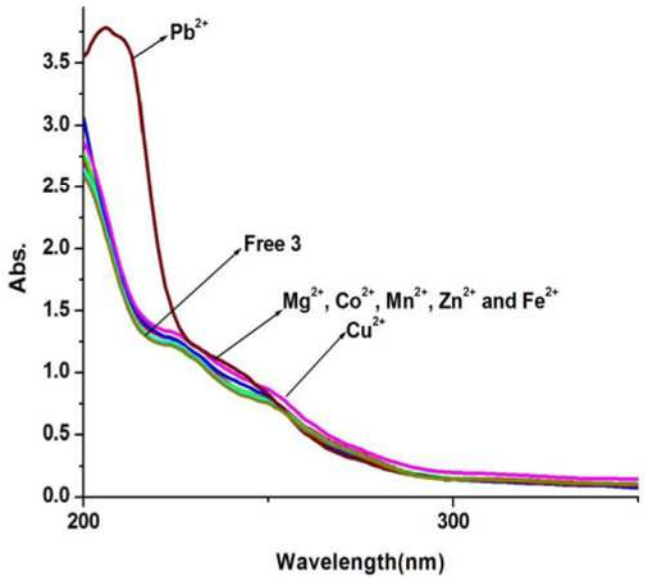

II b. ELECTROCHEMICAL STUDIES

Chemical receptors having ferrocene nuclei as part of the sensing unit have been broadly studied. Earlier, the complexation of ferrocene with different binding site have been studied by cyclic voltammetry, which shows a positive shift of the Fe(II)/Fe(III) redox couple as a result of metal-ligand complexation. The metal-recognition properties of receptor **3** was also evaluated by cyclic (CV) and differential pulse voltammetry (DPV) analysis in CH_3CN solutions containing 0.1 M $[(n\text{-}Bu)_4N]ClO_4$ as supporting electrolyte. All the receptors **3** display a irreversible one-electron oxidation process at $E_{1/2}$ = 0.44 V due to the ferrocene/ferrocenium redox couple. No perturbation of the CV and DPV voltammograms of **3** was observed in presence of other metal cations such as Li^+, Na^+, K^+, Ca^{2+}, Mg^{2+}, Cr^{2+}, Zn^{2+}, Ni^{2+}, Fe^{2+}, Co^{2+}, Tl^+, Cd^{2+} and Pb^{2+} as their appropriate salts. However, as shown in Figure6, the original peak gradually decreased upon stepwise addition of Pb^{2+} ion, while a new peak, associated with the formation of a complexed species, appeared at 0.608 V ($\Delta E_{1/2}$ = 55 mV) for **3** . The net anodic shifts are consistent with the formation of complexed species with Pb^{2+} ion. The linear sweep voltammetry study, LSV Figure6, Supporting Information) further reveals similar results as obtained from CV

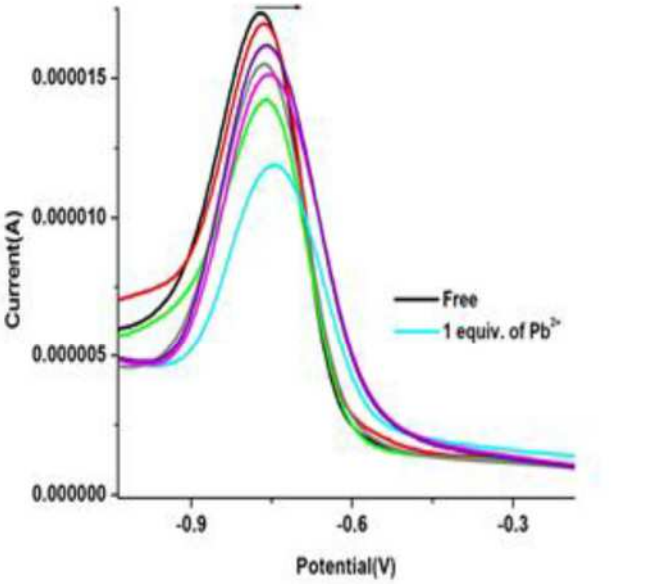

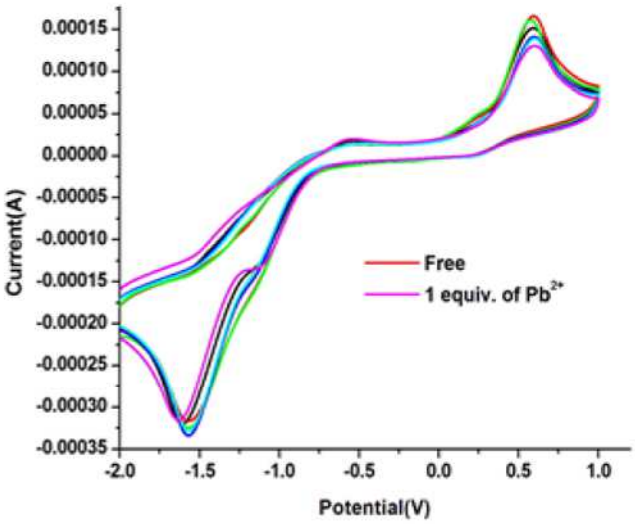

Figure 6. Evolution of LSV (left) and CV (right) of 3 ($1x10^{-4}$ M) upon addition of Pb^{2+} ion up to 1 equiv with $[(n\text{-}Bu)_4N]ClO_4$ as supporting electrolyte. Scan rate employed 0.1 Vs^{-1}.

Figure 6. Evolution of LSV (left) and CV (right) of 3 ($1x10^{-4}$ M) upon addition of Pb^{2+} ion up to 1 equiv with $[(n\text{-}Bu)_4N]ClO_4$ as supporting electrolyte. Scan rate employed 0.1 Vs^{-1}

Intriguingly, as shown in the Figure 6 (left), additional peak has not appeared in CV upon addition of Pb^{2+} ion for compound **4**, only the voltammetric wave shifted towards more cathodic current indicating that the metal cation induces oxidation of the free receptor with its incidental reduction to Cu^{+}. In contrast, when the same experiment carried out upon the addition of Pb^{2+}, a shift of the LSV toward a more positive potential was observed Figure 6, which is in agreement with the complexation process previously observed by CV and DPV

II c .VISUAL RECOGNITION OF PB^{2+} ION

When an excess of different metal ions (Li^{+}, Na^{+}, K^{+}, Ca^{2+}, Mg^{2+}, Cr^{2+}, Zn^{2+}, Ni^{2+}, Co^{2+}, Fe^{2+}, Tl^{+}, Cd^{2+}, and Pb^{2+}) as their perchlorate salts were separately added to a solution of **3** in CH_3CN (10^{-5} M), no significant color change was observed, except for Pb^{2+} and Cu^{2+}. As shown in Figure, Pb^{2+}shows a color change from yellow to brownish yellow, whereas Cu^{2+}shows a color change from yellow to bluish green. This may be due to the oxidation of ferrocene to ferrocenium ion. More remarkably the colorimetric response toward Pb^{2+} is preserved in the presence of water

The absorption spectra changes are responsible for the change of color from yellow to orange that can be used for the selective colorimetric detection of Pb^{2+} in aqueous environment. To support the results obtained by spectro-photochemical experiments and to gain detailed information about the interactions of these metal cation by receptor **3**, we performed the ^{1}H NMR titration-experiments for Pb^{2+} ion. As shown in the Figure 8, the most significant ^{1}H NMR spectral changes observed upon the addition of increasing amounts of Pb^{2+} to a solution of free receptor **3** are the following: the triazole proton (H_a) is significantly shifted.

II d. NMR STUDIES

To support the results obtained by spectro-photochemical experiments and to gain detailed information about the interactions of these metal cation by receptor **3**, we performed the ^{1}H NMR titration-experiments for Pb^{2+} ion. As shown in the Figure 8, the most significant ^{1}H NMR spectral changes observed upon the addition of increasing amounts of Pb^{2+} to a solution of free receptor **3** are the following: the triazole proton (H_a) is significantly shifted.

Figure 7. Evolution of the color in CH_3CN solution of 3 (10^{-5} M) after addition of 5 equiv of different cations tested as perchlorate salt

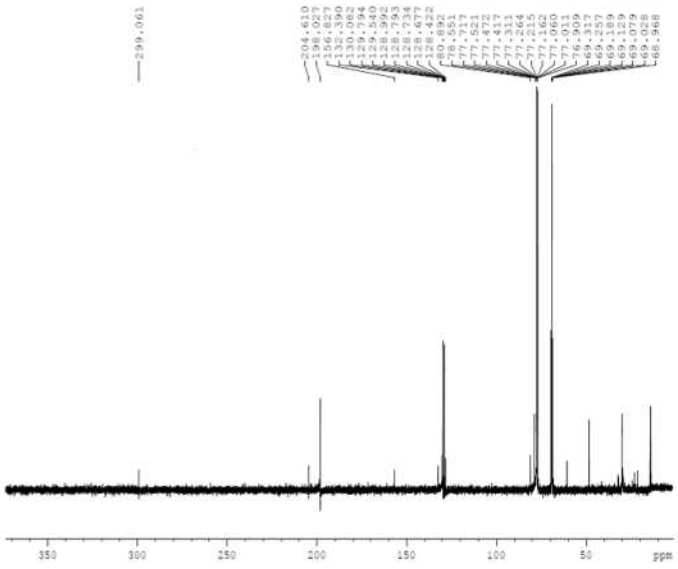

Fig.8.^{1}H NMR titration of 5 upon addition of increasing amount of Pb^{2+} up to 1 equiv

III CONCLUSION

In conclusion, we have described two simple triazole-based, easy-to-synthesize, multisignaling chemosensor 3, which selectively bind with Pb2+ through multiple channels. Interestingly, the redox and colorimetric response toward Pb2+ are preserved in the presence of water, which can be used for the selective colorimetric (naked-eye) detection of Pb2+ in an aqueous environment over other cations, including the strong competitors Ni2+, Hg2+, and Cd2+. To the best of our knowledge, the ferrocene-based ligand 2 is the rare example of a dual electrochemical−optical Pb2+ ion sensor in which the Fc/Fc+ redox couple is significantly shifted (ΔE1/2 = 55 mV) on complexation. with a concomitant change in color from yellow to brownish yellow, that allows its potential use for "naked eye" detection.

REFERENCES

(1) Amarnath Chakraborty, Sujendu Dey, Sudeshna Sawoo,N.N.Sarkar, Amitabha Sarkar,*Organometallics* 2010,29,6619.

(2) Hao-Chih Hung,Chi-Wen Cheng, Yu-Yun Wang,Yu-Jen Chen, Wen-Sheng Chung, *Eur. J. Org. Chem.* **2009**, 6363

(3) Arunabha Thakur, Sundargopal Ghosh, *Organometallics* 2012, 31, 819.

(4) Arunabha Thakur, Dipendu Mandal, Sundargopal Ghosh,*Anal. Chem.* 2013, 85, 1665.

(5) Arunabha Thakur, Sinjinee Sardar, Sundargopal Ghosh, |*Inorg. Chem*. 2011, 50, 7066.

(6) Arunabha Thakur, Dipendu Mandal, Soumik Sao, Sundargopal Ghosh,*Journal of Organometallic Chemistry* 2012,715.

(7) Dipendu Mandal, Arunabha Thakur, Sundargopal Ghosh,*Elsevier Ltd,*2012.

VOLVO'S AUTONOMOUS SELF PARKING CAR

Volvo Car Corporation, known for building safe cars, has been busy expanding its autonomous portfolio.

According to Volvo, the new autonomous concept program would allow drivers to drop their car off near a parking lot in a designated zone, activate the autonomous smart phone app, and the car does the rest. Working off Volvo's modified autonomous technology, the car then seeks out an open parking space and when identified, parks itself and waits for the retrieve command. Once the car has found a spot it sends the owner a notification of its location and that it has parked. Volvo's Vehicle 2 Infrastructure technology in-road sensors are required to inform drivers of drop off locations and activate the system.

To avoid autonomous road rage and traffic incidents, Volvo has programmed the vehicle and its various sensors and cameras to interact in a safe and courteous manner with both pedestrians and competing vehicles. To retrieve the car, owners can either walk to where the car has located itself, or using Volvo's smart phone app signal the car which will then autonomously make its way back to the owner at the designated pick up zone.

Although the system is still conceptual at this point, the accompanying video provides reasonable proof that the autonomous program can function in real world situations. Volvo claims autonomous steering will be available in the 2014 Volvo XC90. Self parking however will remain a hands-on responsibility until Volvo perfects the self-parking technology.

NEW CO2 SAND BRICKS ARE 2.5 TIMES STRONGER THAN CONCRETE

Japanese construction and design firm TIS & Partners has just unveiled a strong and surprisingly low-tech brick that can be rapidly produced in disaster areas, and applied to the quick construction of long lasting shelter. Since the brick's main component is common sand they can be produce in quantity nearly anywhere. The process of making the brick uses carbon dioxide to harden sand and a binder to provide tensile strength. In fact, the inventor claims the bricks are 2.5 times the tensile strength of concrete in one day, meaning that the construction of walls would need much less steel reinforcement and could be used immediately in emergency constructions.

The bricks are created using a very simple process: high silicon content sand is put into an air tight mold that can be virtually any shape. CO2 is pumped into the mold and bonds with the silica to make a solid brick-like material in less than a minute — at this point, the brick is very strong under lateral loads, but still crumbles if stressed under tensile pressure.

The next step is to infuse the bricks with a binder such as epoxy or urethane. Bathing the blocks in the binder creates a hardened block that has all the proper requirements for a strong building component. The brick's strength is 2.5 times that of concrete in less than 24 hours, which is critical for emergency building and predicted to have a 50 year lifespan. The finished bricks can also be more easily transported from where they are locally produce to the building site, and thanks to their tensile strength, they can create walls that require little or no added steel reinforcement. The product also has the promise of being a valuable way to sequester carbon.

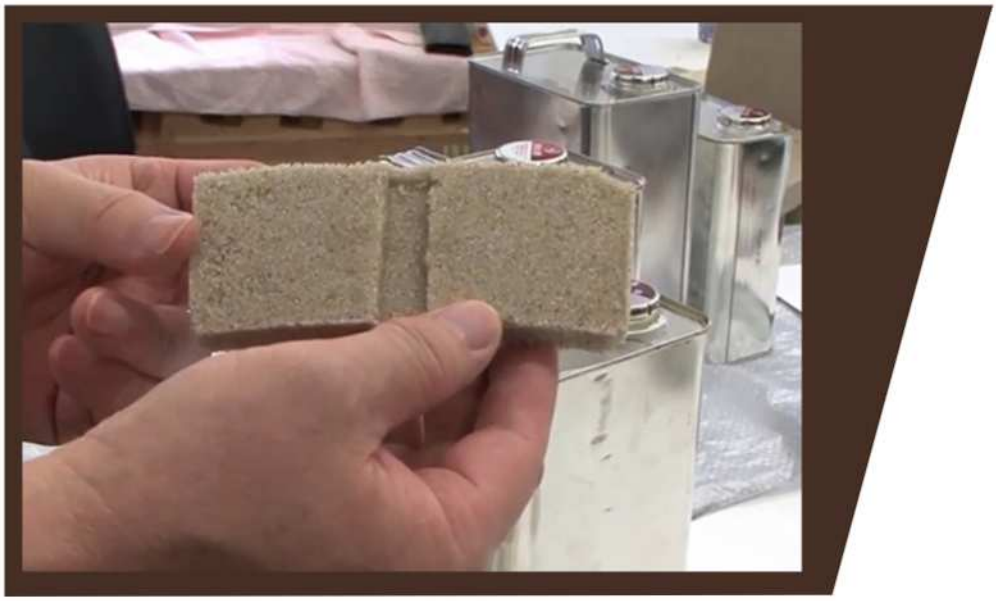

STRETCHY SOLAR CELLS POWER "SUPER SKIN"

The "super skin" developed by Stanford University researcher Zhenan Bao is self-powering, using polymer solar cells to generate electricity. The solar cells are not just flexible, but stretchable -- they can be stretched up to 30 percent beyond their original length and snap back without any damage or loss of power. Bao, a professor of chemical engineering, presented her work on Feb. 20 at the AAAS annual meeting in Washington, D.C.

The foundation for the artificial skin is a flexible organic transistor, made with flexible polymers and carbon-based materials. To allow touch sensing, the transistor contains a thin, highly elastic rubber layer, molded into a grid of tiny inverted pyramids. When pressed, this layer changes thickness, which changes the current flow through the transistor. The sensors have from several hundred thousand to 25 million pyramids per square centimeter, corresponding to the desired level of sensitivity.

To sense a particular biological molecule, the surface of the transistor has to be coated with another molecule to which the first one will bind when it comes into contact. The coating layer only needs to be a nanometer or two thick.

Bao's team has successfully demonstrated the concept by detecting a certain kind of DNA. The researchers are now working on extending the technique to detect proteins, which could prove useful for medical diagnostics purposes.

"For any particular disease, there are usually one or more specific proteins associated with it -- called biomarkers -- that are akin to a 'smoking gun,' and detecting those protein biomarkers will allow us to diagnose the disease," Bao says. The same approach would allow the sensors to detect chemicals, she said. By adjusting aspects of the transistor structure, the super skin can detect chemical substances in either vapor or liquid environments.

Regardless of what the sensors are detecting, they have to transmit electronic signals to get their data to the processing center, whether it is a human brain or a computer.

Having the sensors run on the sun's energy makes generating the needed power simpler than using batteries or hooking up to the electrical grid, allowing the sensors to be lighter and more mobile. And having solar cells that are stretchable opens up other applications.

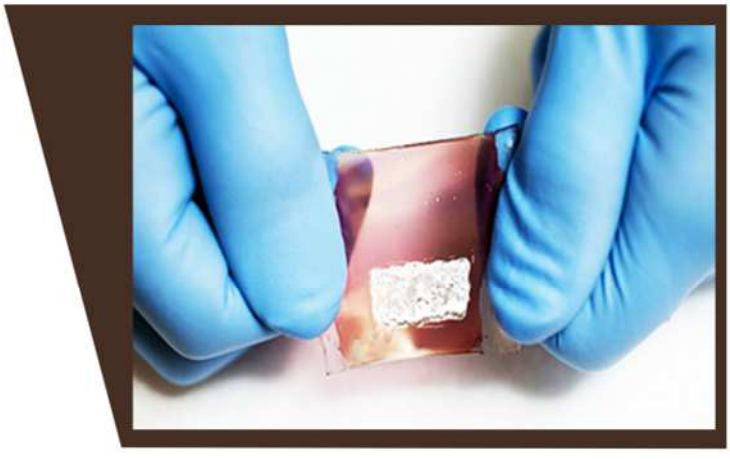

3 DIMENSIONAL PRINTING

Imagine a future in which a device connected to a computer can print a solid object. A future in which we can have tangible goods as well as intangible services delivered to our desktops or highstreet shops over the Internet. And a future in which the everyday "atomization" of virtual objects into hard reality has turned the mass pre-production and stock-holding of a wide range of goods and spare parts into no more than an historical legacy.

Such a future may sound like it is being plucked from the worlds of Star Trek. However, while transporter devices that can instantaneously deliver us to remote locations may remain a fantasy, 3D printers capable of outputting physical objects have been in development for over two decades and are starting to present a whole host of new digital manufacturing capabilities. 3D printing may therefore soon do for manufacturing what computers and the Internet have already done for the creation, processing and storage of information. Such a possibility has also started to capture mainstream media attention.

A 3D printing technology that creates objects by using a light source to solidify a liquid photopolymer is known generically as 'material jetting', or commercially as 'polyjet matrix'. This was pioneered by a company called Objet (now a part of Stratasys), and forms object layers by emitting liquid photopolymer from an inkjet-style, multi-nozzel print head. After each layer is printed a powerful UV light is then used to set it solid before the next layer is printed. The really clever thing is that the Connecx range of 3D printers created by Objet can jet several different materials from their print head, and in varying combination. This allows up to 14 of 120 potential materials to be printed at the same time.

Another category of 3D printer hardware is based on material extrusion. Here a semi-liquid material -- and most usually a hot thermoplastic -- is deposited from a computer-controlled print head. This process was invented by Scott Crump in 1988, who set up a company called Stratasys to commercialize his invention. Crump chose to name the technology 'fused deposition modelling' or 'FDM', and patented and trademarked these terms. Hence, while many people use the phrase 'FDM' to refer to this kind of 3D printing, only Stratasys actually makes FDM 3D printers. Others manufacturers refer to the same process as 'thermoplastic extrusion','plastic jet printing' (PJP), the 'fused filament method' (FFM) or 'fused filament fabrication' (FFF)

Whatever it is called, one of the key benefits of FDM is that objects can be made of out of exactly the same thermoplastics used in traditional injection moulding.

iOS 7

Apple revealed that its next-generation mobile operating system will be released on September 18, 2013 and Enterprise users and IT administrators should note several new features that will make iPhones and iPads more secure and easier to manage in corporate environments. In addition, iOS 7 offers some new ways to configure and deploy devices at scale, and has new features to help businesses purchase, distribute, and manage apps.

Perhaps the biggest new enterprise feature is the iPhone 5S' fingerprint identity sensor, which while technically hardware, is enabled by new software features in iOS 7. Branded as the Touch ID fingerprint reader and invisibly embedded in the home button, this 500ppi fingerprint sensor can keep enterprise data more secure than ever. Touch ID brings two-factor authentication to the iPhone, combining something you know (i.e. a passcode) with something you have (your fingerprint) to increase security.

As detailed in its iOS 7 for business webpage, Apple's new OS has several offerings that will appeal to Enterprise users and administrators:

"Open in..." management

When you touch an email attachment on an iPhone you'll see the familiar "open in..." option which allows you to choose which app opens said attachment. iOS 7 allows business to protect corporate data by controlling which apps (and accounts) are used to open documents and attachments. This keeps work documents in corporate apps and also prevents personal documents from being opened in managed apps.

Enterprise single sign on

Enterprise single sign on (SSO) means user credentials can be used across apps, including apps from the App Store. Each new app configured with SSO verifies user permissions for enterprise resources, and logs users in without requiring them to re-enter passwords.

Mobile Device Management (MDM)

The new MDM protocol in iOS 7 includes several commands, queries, and configuration options that make third-party MDM solutions even more powerful. With iOS 7 MDM IT administrators can set up managed apps, install custom fonts, configure accessibility options and AirPrint printers, and whitelist AirPlay destinations over the air.

But that's not all!

Apple has also added Streamlined MDM enrollment, improved App Store license management, third-party app data protection, improved mail and support for Caching Server 2 into iOS 7, making it the most manageable and secure mobile OS on the planet.

8 FACTS ABOUT STEPHEN HAWKING

From some of his scientific beliefs to works he's written, there are a few things you might not have guessed about world renowned physicist Stephen Hawking.

1.) Received Mediocre Grades in School

Even if you don't keep a close eye on new developments in physics, you've probably heard of the renowned physicist Stephen Hawking. He's prided himself on making his complex physical concepts accessible to the public and writing the bestseller, "A Brief History of Time." And if you are a fan of Conan O'Brien, "The Simpsons" or "Star Trek," you might have seen him brandishing his cool wit during guest appearances on those shows.

Even if you are familiar with his academic work, however, there are many interesting facts you might not know about Hawking, stretching from his time at school and gradual development of disability to his opinions on the future of the human race.

Many find it surprising, for instance, that, despite his influential body of work, Hawking hasn't yet been awarded the Nobel Prize. We'll talk about some of the remarkable distinctions he has received, however.

Another interesting fact: Hawking was born on Jan. 8, 1942, which just happened to be the 300th anniversary of Galileo's death.

But this has just been the warm-up. Next, we'll delve into some fascinating and unexpected facts about Hawking, including some things about his profoundly inspirational story.

These days, we know Hawking as a brilliant mind whose theories are difficult for a nonscientific mind to grasp. This is why it may come as a shock to learn that Hawking was a slacker when it came to his school studies. In fact, when he was 9 years old, his grades ranked among the worst in his class [source: Larsen]. With a little more effort, he brought those grades up to about average, but not much better.

Nevertheless, from an early age he was interested in how stuff worked. He has talked about how he was known to disassemble clocks and radios. However, he admits he wasn't very good at putting them back together so they could work again.

Despite his poor grades, both his teachers and his peers seemed to understand that they had a future genius among them, evidenced by the fact that his nickname was "Einstein." The problem with his mediocre grades was that his father wanted to send him to Oxford, but didn't have themoney without a scholarship. Luckily, when it came time for the scholarship exams, he aced them, getting an almost perfect score on the physics exam.

2.) Had an aversion to biology.

Stephen Hawking took a liking to mathematics from an early age, and he would have liked to have majored in it. His father, Frank, however, had different ideas. He hoped Stephen would instead study medicine.

But, for all his interest in science, Stephen didn't care for biology. He has said that he found it to be "too inexact, too descriptive" [source: Larsen]. He would have rather devoted his mind to more precise, well-defined concepts.

One problem, however, was that Oxford didn't have mathematics as a major. The compromise was that Stephen would attend Oxford and major in physics.

In fact, even within physics, he focused on the bigger questions. When faced with deciding between the two tracks of particle physics, which studies the behavior of subatomic particles, versus cosmology, which studies the large universe as a whole, he chose the latter. He chose cosmology despite the fact that, at that time, he says, it was "hardly 4recognised as a legitimate field" [source: Hawking].

In explaining why, he said that particle physics "seemed like botany. There were all these particles, but no theory"

3.) Was on Oxford Rowing Team.

Biographer Kristine Larsen writes about how Hawking faced isolation and unhappiness during his first year or so at Oxford. The thing that seems to have drawn him out of this funk was joining the rowing team.

Even before being diagnosed with a physically disabling illness, Hawking didn't have what one would call a large or athletic build. However, row teams recruited smaller men like Hawking to be coxswains -- a position that does not row, but rather controls steering and stroke rate.

Because rowing was so important and competitive at Oxford, Hawking's role on the team made him very popular. Remembering Hawking from those days, one fellow boatsman called him "the adventurous type" [source: Larsen].

But as much as the rowing team helped his popularity, it hurt his study habits. Occupied with rowing practice for six afternoons per week, Hawking started "to cut serious corners" and used "creative analysis to create lab reports"

A NUCLEAR CLOUD

When asked why she was willing to marry him, Jane said that in those times they lived under the "most awful nuclear cloud -- that with a four minute warning the world itself could likely end." She says they wanted "to make the most of whatever gifts were given us"

4.) Was given a few years to live at age 21.

As a graduate student, Hawking gradually started showing symptoms of tripping and general clumsiness. His family became concerned when he was home during his Christmas break from school and they insisted he see a doctor.

Before seeing a specialist, however, he attended a New Year's party where he met his future wife, Jane Wilde. She remembers being attracted to his "his sense of humor and his independent personality."

He turned 21 a week later, and shortly after he entered the hospital for two weeks of tests to discover what was wrong with him. He was then diagnosed with amyotrophic lateral sclerosis (ALS), also known as Lou Gehrig's disease, which is a neurological disease that causes patients to lose control of their voluntary muscles. He was told he'd probably only have a few years to live.

Hawking remembers being shocked and wondering why this happened to him. However, seeing a boy dying of leukemia in the hospital made him realize that there were others worse off than him.

Hawking became more optimistic and started dating Jane. They were soon engaged, and he cites their engagement as giving him "something to live for" [source: Larsen].

5.) Helped create the Boundless Universe Theory

One of Hawking's major achievements (which he shares with Jim Hartle) was to come up with the theory that the universe has no boundaries in 1983.
In 1983, the effort to understand the nature and shape of the universe, Hawking and Hartle combined the concepts of quantum mechanics (the study of the behavior of microscopic particles) with general relativity (Einstein's theories aboutgravity and how mass curves space) to show that the universe is a contained entity and yet has no boundaries.
To conceptualize this, he tells people to think of the universe like the surface of the Earth. As a sphere, you can go in any direction on the surface of the Earth and never reach a corner, an edge or any boundary where the Earth can be said to "end." However, one major difference is that the surface of the Earth is two-dimensional (even though the Earth itself is three-dimensional, the surface is only two-dimensional), while the universe is four-dimensional.
Hawking explains that spacetime (see the sidebar on this page) is like the lines of latitude on the globe. Starting at the North Pole (the beginning of the universe) and going south, the circumferences get bigger until beyond the equator, when they would get smaller. This means that the universe is finite in spacetime and will re-collapse eventually -- however, not for at least 20 billion years [source: Hawking]. Does this mean that time itself would go backwards? Hawking grappled with this question, but decided no, because there is no reason to believe that the universe's trend from ordered energy into disordered energy will reverse.

6.) Lost a bet on Black Holes.

In 2004, the genius Hawking admitted he had been wrong and conceded a bet he made in 1997 with a fellow scientist aboutblack holes. To understand the bet, let's backpedal a little to understand what black holes are in the first place.
Stars are gigantic -- they have so much mass that their gravityis always incredibly strong. This is fine, as long as the starcontinues to burn its nuclear fuel, exerting this energy outward, thus counteracting gravity. However, once a massive enough star "dies" or burns out, gravity becomes the stronger force, and causes that big star to collapse on itself. This creates what scientists call a black hole.

INSEPERABLE BUDDIES : SPACE AND TIME
Time also fits into the Earth comparison. Because Einstein showed that space and time are relative to each other, physicists measure them together in sp cetime. And, because of this relationship and mathematical servations showing the universe is expanding, physicists believe time is affected by the expansion of the universe.

The gravity is so powerful in this collapse that not even light can escape. However, Hawking proposed in 1975 that black holes are not really black. Rather, they radiate energy.
But, he said at the time, information is lost in the black hole that eventually evaporates. The problem was that this idea that information is lost conflicted with the rules of quantum mechanics, creating what Hawking called an "information paradox."
American theoretical physicist John Preskill disagreed with this conclusion that information is lost in black hole. In 1997, he made a bet with Hawking saying that information can escape from them, thus not breaking the laws of quantum mechanics.
Hawking is such a good sport that he can admit when he's wrong -- which he did in 2004. While giving a lecture at a scientific conference, he said that because black holes have more than one "topology," and when one measures all the information released from all topologies, information isn't lost.

7.) Believes in the possibility of Aliens.

Considering all of Hawking's work in cosmology, people are understandably interested in his opinions on the possibility of alien life. During NASA's 50th anniversary celebration in 2008, Hawking was invited to speak, and he mentioned his thoughts on the subject.
He expressed that, given the vastness of the universe, there very well could be primitive alien life out there, and it is possible, other intelligent life.
"Primitive life is very common," Hawking said, "and intelligent life is very rare." Of course, he threw in his characteristically sharp humor to say, "Some would say it has yet to occur onEarth" [source: Hawking]. He went on the say that humans should be wary of exposure to aliens because alien life will probably not be DNA-based, and we would not have resistance to diseases.
Hawking also did an episode on the possibility of aliens for "Into the Universe with Stephen Hawking" on the Discovery Channel (the parent company of HowStuffWorks.com).
In this episode, he explains that aliens might use up their own planet's resources and "become nomads, looking to conquer and colonize whatever planets they could reach." Or, they could set up a mirror system to focus all the energy of the sun in one area, creating a wormhole -- a hole to travel through spacetime.

8.) Took Zero Gravity flight to save human race.

In 2007, when Stephen Hawking was 65 years old, he got to take the ride of a lifetime. He was able to experience zero-gravity and float out of his wheelchair thanks to Zero Gravity Corp. The service involves an airplane ride in which sharp ascent and descent allows passengers to experience weightlessness in flight for several rounds, each about 25 seconds long.
Hawking, free from his wheelchair for the first time in four decades, was even able to perform gymnastic flips. Hawking also has booked a seat with Richard Branson's Virgin Galactic to ride on a sub-orbital flight.
But perhaps most interesting about this is not what he was able to do, but why he did it. When asked about why he wanted to do this, he of course cited his desire to go into space. But his reasons for going and his overall support for space travel went deeper than that.
Due to the possibility of global warming or nuclear war, Hawking has said that the future of the human race, if it is going to have a long one, will be in outer space [source: Boyle]. He supports private space exploration in hopes that space tourism will become affordable for the public. He hopes that we can travel to other planets to use their resources to survive.

A SINGULAR EVENT.
A singularity is a point of spacetimewhere Einstein's idea of general relativity breaks down because the gravitational forces are so strong. Theoretical physicists believe this happens when a black hole is formed, and may have happened at the creation of our universe. Hawking's No-Boundary Proposal, however, suggests the world did not begin in a singularity.

We would like to thank Vishwanath Sivaramakrishnan , Srivatsa Bommu, and Navneet Vinod Kumar for igniting and inspiring us for this initiative.

Compiled by:
- *Luvy Arora*
- *Shashank Peri*
- *GSV Harshavardhan*
- *Varun Vijay*
- *Rishiraj Singh*
- *Dhiren Balasaria*
- *Anirudh Mani*
- *Sri Harsha Sivanapalli*
- *Hassan Bohra*

Design By:
- *Aditya Ekka*
- *Aditya Singh*